Computational Optimization and Experimental Evaluation of Grasp Quality for Tendon-Driven Hands Subject to Design Constraints

Joshua M. Inouye
Multiscale Muscle Mechanics Lab,
Department of Biomedical Engineering,
University of Virginia,
Charlottesville, VA 22902
e-mail: jmi@virginia.edu

Francisco J. Valero-Cuevas
Brain-Body Dynamics Lab,
Department of Biomedical Engineering &
the Division of Biokinesiology and
Physical Therapy,
University of Southern California,
Los Angeles, CA 90089
e-mail: valero@usc.edu

The chief tasks of robotic and prosthetic hands are grasping and manipulating objects, and size and weight constraints are very influential in their design. In this study, we use computational modeling to both predict and optimize the grasp quality of a reconfigurable, tendon-driven hand. Our computational results show that grasp quality, measured by the radius of the largest ball in wrench space, could be improved up to 259% by simply making some pulleys smaller and redistributing the maximal tensions of the tendons. We experimentally evaluated several optimized and unoptimized designs, which had either 4, 5, or 6 tendons and found that the theoretical calculations are effective at predicting grasp quality, with an average friction loss in this system of around 30%. We conclude that this optimization can be a very useful design tool and that using biologically inspired asymmetry and parameter adjustments can be used to maximize performance.
[DOI: 10.1115/1.4025964]

1 Introduction

Robotic and prosthetic hands have been designed for many years, and their essential tasks are grasping and manipulating objects [1–12]. Many robotic and prosthetic hands also are designed with approximately the same shape and/or size as the human hand in order to be able to perform tasks in place of a human. Weight and size constraints are two of the paramount design constraints for these manipulators. Actuators for the fingers, typically located proximal to the hand, are generally either larger or heavier if they are able to produce more tension. This is also the case in the human hand: larger muscles are both heavier and stronger. In addition, the pulley sizes in the fingers cannot be made too big, otherwise, the finger itself will become too large. In this paper, we utilize two reconfigurable fingers to test computational predictions of grasp quality for a given tendon routing, whose pulley sizes are constrained and the sum of maximal tendon tensions is constrained (due to weight and size constraints on the actuation system).

In addition to maximizing performance for a set of given constraints, the optimization techniques presented here can also be used to minimize size or weight given performance requirements. This is a useful tool when designing certain tendon-driven systems, such as minimally invasive surgical devices (minimization of size and number of actuators desired) and prosthetic hands (minimization of weight desired). The consequences of overdesigning the capabilities of these systems are increased weight, cost, size, and power consumption. Other capabilities important in the design of these systems are position control, force control, velocity production, and design simplicity.

A large body of literature exists which addresses grasp quality of objects by robotic hands and manipulators. Some studies have looked at grasp quality in order to determine the optimal finger placement on an object by a robotic hand [13–16]. However, they do not take into account the mechanical capabilities of the fingers and therefore are only useful in optimizing grasp placement and hand kinematics, not in optimizing the design parameters. Mechanical design parameters were taken into account for tendon-driven hands in Ref. [17], but they did not optimize over the parameters. Optimization of parameters given requirements on force production for a single finger was examined in Ref. [18], but they did not implement any of the optimized designs in hardware, and they did not optimize for grasp quality. The hardware implementation of robotic hands has been widely accomplished [1–12], but their choice of design parameters has not been guided by a systematic optimization or analyses of grasp quality.

Our study uses a previously developed computational framework [19] to evaluate and optimize the grasp quality of a reconfigurable tendon-driven hand (taking into account all design parameters and constraints). The mechanical design of the reconfigurable fingers is identical to that of a finger used in another study for single finger force-production analysis and optimization [20]. We show that under specific geometric and design constraints, optimization of design parameters can improve grasp performance by more than 200%, and our predictions of grasp quality are corroborated by experimental results.

2 Methods

2.1 Hand Construction. The robotic hand we optimized and tested consisted of two reconfigurable fingers, which were designed for a previous study [20]. 2-D views of the finger design are shown in Fig. 1. The fingers were able to accept arbitrary tendon routings that were analyzed and optimized computationally. In addition, the pulley size was variable, consisting of two options: a large pulley, with radius 8 mm, and a small pulley, with radius 4.4 mm. Each of the custom pulleys was fitted with ball bearings to minimize friction.

2.2 Grasp Quality Analysis and Definition of Fitness Function. Our calculation of grasp quality was based on the wrench-direction-independent metric known as the radius of largest ball

Contributed by the Mechanisms and Robotics Committee of ASME for publication in the Journal of Mechanical Design. Manuscript received July 8, 2013; final manuscript received October 18, 2013; published online December 11, 2013. Assoc. Editor: Oscar Altuzarra.

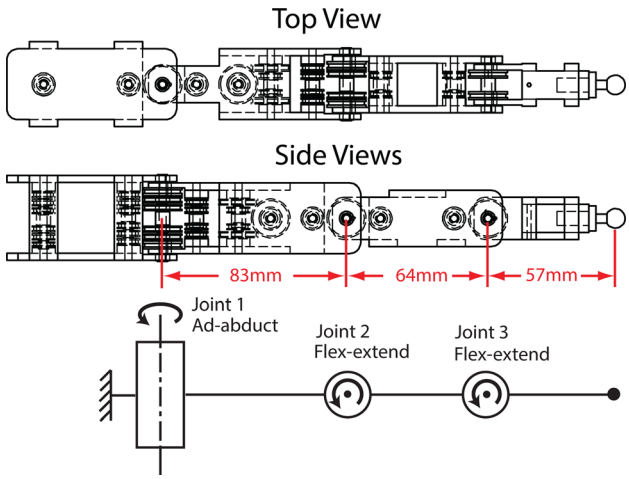

Fig. 1 Top and side views of finger design and kinematics

[21,22]. The metric, in effect, is equal to the maximal magnitude of a wrench that can be applied to the object in all directions in wrench space without it losing force closure (i.e., causing the grasp to fail). A wrench vector whose magnitude is less than the grasp quality can be applied to the object *in any direction in wrench space* without losing force closure. The process for efficiently calculating the grasp quality and optimizing the parameters of a tendon-driven hand was originally developed in Ref. [19].

Briefly, the grasp quality analysis first involves selecting the initial grasp parameters: the finger geometry and posture, object size and shape, grasping points, and number of fingers. These are defined for this experiment as shown in Fig. 2. We analyzed grasp quality for two different finger placements, also in Fig. 2. Next,

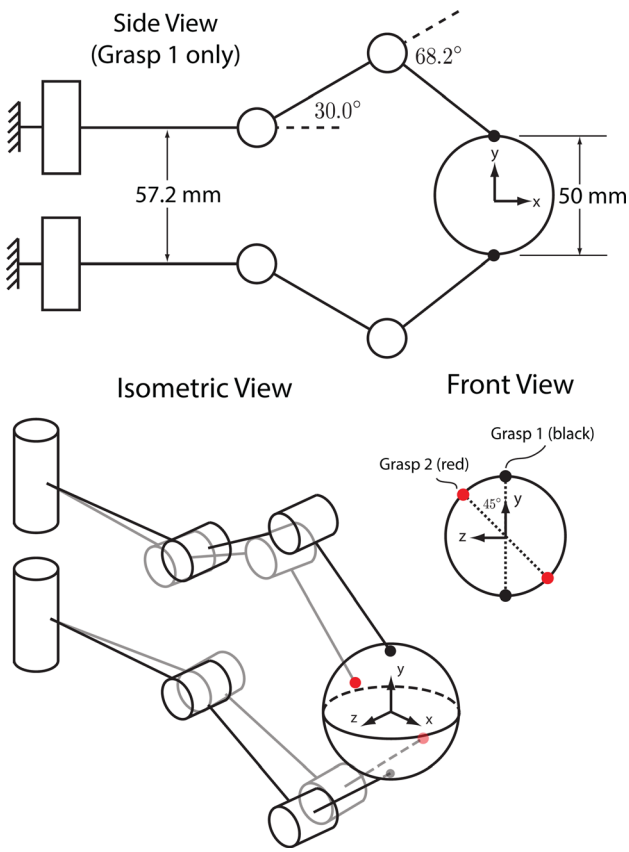

Fig. 2 Finger placements for each grasp

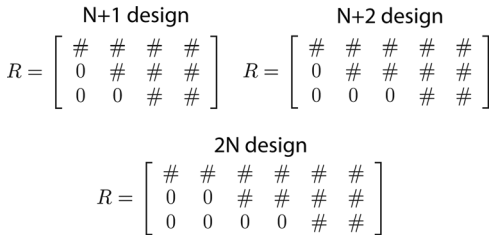

Fig. 3 Base moment arm matrices used when finding realizable, unique tendon routings

the fingertip force-production capabilities for each finger are determined by calculating the feasible force set, which is a function of finger posture and geometry, tendon routing and pulley sizes, and maximal tensions of the tendons [23]. The finger Jacobian, J, relating joint angle velocities to endpoint velocities, is determined from the geometry (i.e., D-H parameters) of the finger and the finger posture. The tendon routing and pulley sizes determine the moment arm matrix R. The maximal tensions of the tendons define the diagonal F_0 matrix. After the feasible force sets are calculated, they are intersected with friction cones, whose orientation is dependent on fingertip contact angle in order to produce a feasible object force set. We used a coefficient of friction of 0.5 for this study. This set represents the forces that can be applied to the object by the fingertip. The feasible object force set is calculated for each finger, using the finger placements determined initially. These sets are used to determine all the forces and torques that can be resisted in wrench space (i.e., the grasp wrench set), from which the grasp quality metric is then calculated using the Quickhull algorithm [24] implemented in the software program Qhull.

The construction of the finger allowed for various moment arm matrices (which define the tendon routing and pulley sizes of the finger) to be implemented which had 4, 5, or 6 tendons. These designs are known as N+1, N+2, and 2 N designs, where N is the number of kinematic degrees of freedom of the finger. We enumerated all possible moment arm matrices beginning with the "base" matrices shown in Fig. 3. We replaced each "#" with either a 1 or −1 (in accordance with the sign of the moment exerted on a joint when the corresponding tendon is under tension; see Fig. 1 for definition of joint axes) in a full combinatoric search and then checked the controllability conditions as described in Ref. [25]. We checked if the matrix was full rank, made sure there was at least one sign change in each row (i.e., that each joint had an extensor and flexor tendon) and tested if a null-space basis vector found via singular value decomposition existed, whose elements all had the same sign (to make sure the finger could hold a posture). This resulted in a total of 252 realizable, unique routings (all with large moment arms): 12 N+1 routings, 80 N+2 routings, and 160 2 N routings. The construction of the finger only allowed for routings where the tendons routed around every joint that they passed (i.e., that the moment arm matrix is pseudo-triangular, as in Ref. [25]).

We then calculated the grasp quality for these routings using the large pulleys and an even distribution of maximal tendon tension. The sum of maximal tendon tensions was limited to 60 N for each finger[1] (i.e., for designs with 4, 5, and 6 tendons, the maximal tensions were 15 N, 12N, and 10N, respectively).

[1]The sum of maximal tendon tensions being equal is an important constraint due to the size, weight, and motor torque (and therefore tendon tension) limitations inherent in dextrous hands. For example, the torque capacity of motors is roughly proportional to motor weight, and minimization of weight was an important consideration in the design of the DLR Hand II [26]. In addition, the maximal force production capabilities of McKibben-style muscles are roughly proportional to cross-sectional area [18]. Since the actuators typically will be located in the forearm, then the total cross-sectional area will be limited to the forearm cross-sectional area. In this study, we do not consider alternative constraints on the actuation system (e.g., electrical current capacity, tendon velocities, etc).

2.3 Optimization of Grasp Quality. The fitness metric we used for optimization was the sum of the grasp qualities for Grasp 1 and Grasp 2 (they were both weighted equally), as defined above.

2.3.1 Optimizing Pulley Sizes. We calculated the fitness for all combinations of large and small pulleys for the best routing from each of the base moment arm matrices shown in Fig. 3. We also optimized the moment arms for the following naive 2N design (where 1 and −1 denote the large moment arm sizes), for a total of 4 pulley-size-optimized routings:

$$R_{\text{NAIVE 2N}} = \begin{bmatrix} 1 & -1 & 1 & -1 & 1 & -1 \\ 0 & 0 & 1 & -1 & 1 & -1 \\ 0 & 0 & 0 & 0 & 1 & -1 \end{bmatrix}$$

A combinatoric search for the 2N designs involved 12 moment arms, so $2^{12} = 4096$ fitness evaluations were performed. Similarly, the N+2 design had 2048 evaluations and the N+1 design had 512 evaluations.

2.3.2 Optimizing Distribution of Maximal Tendon Tensions. The last step in our optimization process involved performing a greedy Markov-Chain Monte Carlo algorithm on the maximal tendon tension distribution. Starting with all the tendons having equal maximal tendon tensions, we perturbed the distribution of the maximal tendon tensions using a multivariate normal distribution with standard deviation of 1% of the maximal tendon tension sum. This perturbation was effectively like one inside an n-dimensional hypercube in the positive orthant with side length equal to maximal tendon tension sum, where n is the number of tendons for each finger. After perturbation inside the hypercube, we projected the point onto the hyperplane given by the following equation:

$$\sum_{i=1}^{n} F_{i,\max} = \text{MaxTendonTensionSum} \tag{1}$$

where $F_{\text{i,max}}$ is the maximal tension of tendon i and one of the diagonal entries in the F_0 matrix. This would give us a new distribution of maximal tendon tensions, and we would then evaluate the fitness. If it was higher, we would take that point as the starting point for the next perturbation. The maximal tendon tensions were constrained so that they did not go negative or above the total maximum, and a reflection technique at those boundaries was used similar to that in Ref. [27]. The overall process is shown graphically for a simplified 2-tendon example in Fig. 4.

A detailed explanation of the effects of different structure matrices and distributions of maximal tendon tensions on the kinetostatic (i.e., force-production) capabilities of manipulators and biological hands can be found in Refs. [19,23,25,28–31].

2.4 Experimental Testing of Tendon Routings. We tested each of the pulley-size-optimized layouts for each of the 4 routings (the best from each of the base matrices, and then the naive 2N). We tested them with optimized tendon tension distributions and unoptimized tendon tension distributions. This gave 8 finger design configurations, and we tested each of these 8 designs in both grasp configurations. This gave 16 tests. In addition, we tested the naive 2N design in both postures with unoptimized pulley sizes and unoptimized tendon tension distribution. So we obtained a total of 18 data points.

2.4.1 Tendon Routing and Actuation. For each of the designs tested, we first arranged the pulleys and strings (0.4 mm braided polyester twine) to match the desired configuration. We then mounted the fingers onto a base that was part of a motor array system as shown in Fig. 5. The DC motors were coupled to shafts which string wound around. The string was then routed around pulleys that were attached to Interface SML 25 load cells which

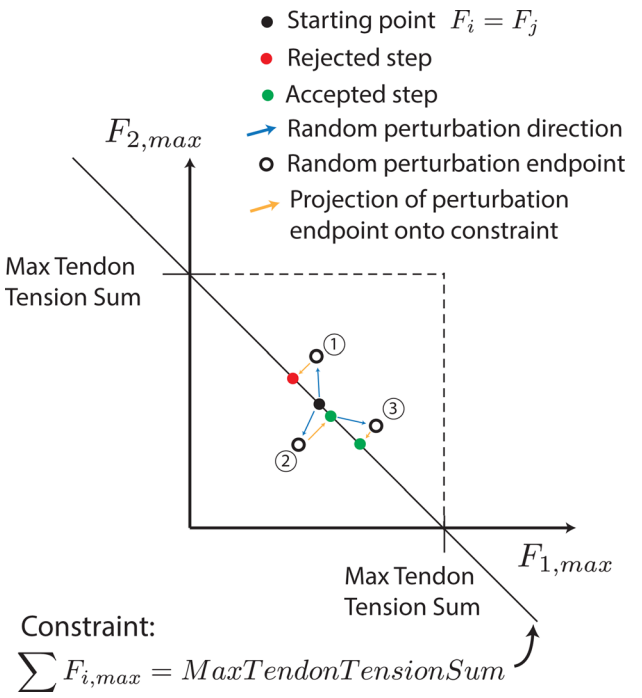

Fig. 4 Illustration of Markov-Chain Monte Carlo algorithm for distribution of maximal tendon tensions

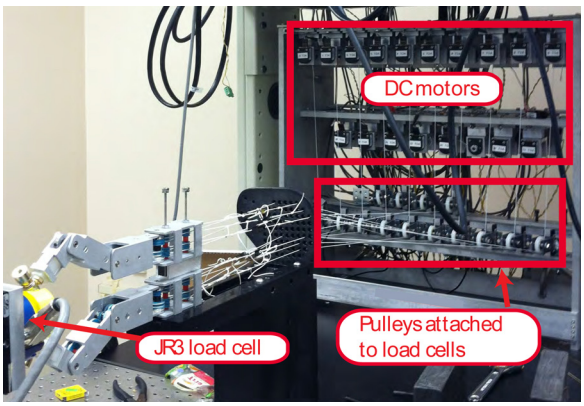

Fig. 5 Experimental system for grasp testing

provided force measurements for the closed-loop controller implemented in LabView.

2.4.2 Test Object. The ends of the fingers had a ball which fit into a socket on the object that we designed to attach to the 6-axis JR3 load cell and also provide the correct finger placements, as seen in the close-up Fig. 6(*a*). Figure 6(*b*) shows the ball-and-socket joints locked into place for grasp configurations 1 and 2. This ball-and-socket joint constrained translational motion but not rotational motion.[2] One object was printed for each grasp configuration. Both are shown in Fig. 5. The sampling rate and control loop frequency were both 100 Hz.

2.4.3 Test Methodology. A small pretension of 1N was applied to each string to remove slack and prevent the string from falling off of the pulleys. Then the Minkowski sum[3] of each

[2]This defined a point-contact with friction, which is needed to match the mathematical framework of the analysis as it does not make the system over-constrained [32].

[3]The Minkowski sum in this context refers to the combination of each vertex of one feasible object force set with every vertex of the other feasible object force set.

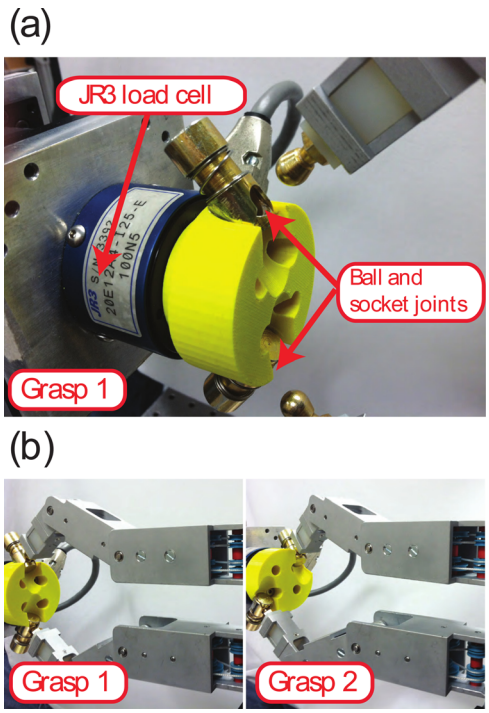

Fig. 6 (*a*) We used a ball-and-socket joint to hold the fingers in place. (*b*) Experimental grasps 1 and 2 are shown as depicted in Fig. 2

vertex of both feasible object force sets (described in the previous section) was applied to the strings (in addition to the pretension) in ramp-up, hold, and ramp-down phases to find the grasp wrench set. The vertices of this experimental grasp wrench set were determined from the hold phases and then used to find the grasp quality. The experimental grasp quality could then be compared with the theoretical grasp quality (from computational results), with the fitness function defined as in Sec. 2.2.

3 Results

3.1 Computational Optimization of Grasp Quality. The 252 unoptimized routings produced the grasp qualities shown in

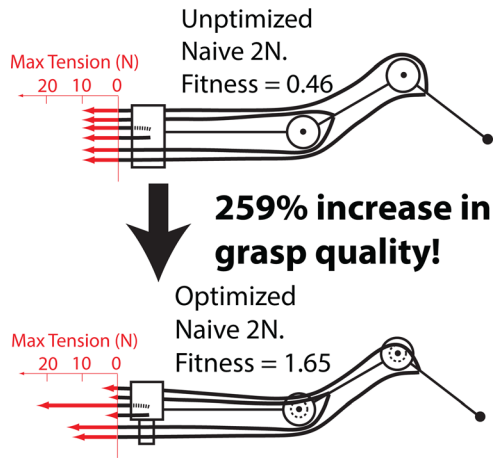

Fig. 8 Computational predictions of fitness for unoptimized and optimized naive 2N design

Fig. 7. The optimization paths for the best N+1, N+2, and 2N designs, plus the naive 2N design, are also shown. Each optimization step produced a higher fitness, and iso-fitness dashed lines are shown.

We see that the naive 2N design improved the most from the optimization steps. This would be expected since the other designs that were optimized already had the highest fitness from their base matrix. That is, they were optimized already to a fair extent by changing the base matrix, while already having large moment arms and equal maximal tensions. The naive 2N design stood the most to gain from the other optimization steps due to its poor initial fitness. In fact, the naive 2N design improved its fitness by 259%. We see the optimization for the naive 2N design made 6 out of the 12 moment arms smaller and redistributed the maximal tensions severely, as seen in Fig. 8.

Furthermore, we can see that the optimized N+1 design had a fitness that was higher than *any* of the unoptimized N+2 and 2N designs, even though it had fewer tendons. Fewer tendons, in general, would be desirable due to simplification of the actuation system and less complexity in design and manufacturing.

3.2 Theoretical Predictions vs. Experimental Results. As would be expected from frictional losses and experimental

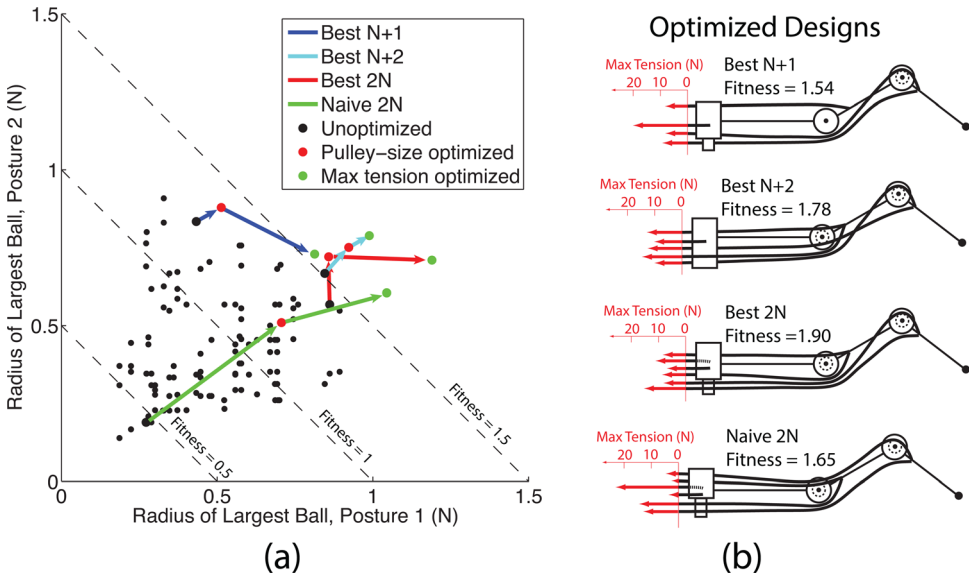

Fig. 7 Computational results of grasp quality for hand designs. (*a*) Optimization paths shown. (*b*) Final optimized designs indicating pulley-size and maximal tendon tension

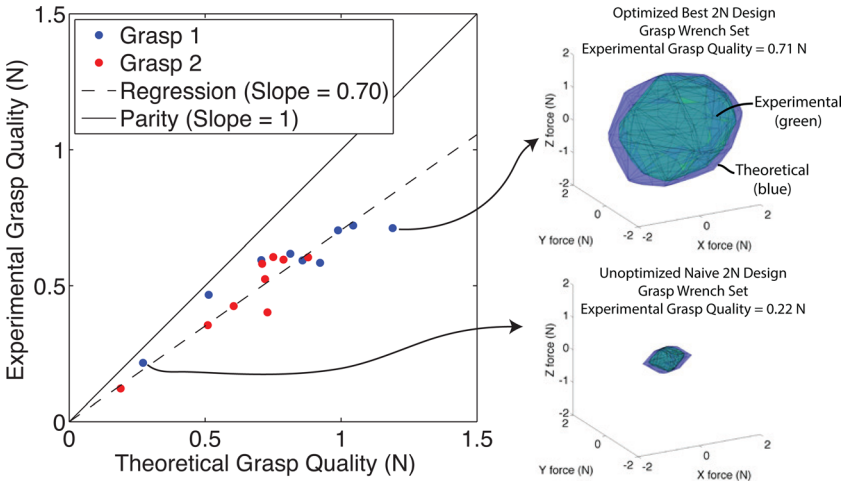

Fig. 9 Results from experimental testing of various routings. Experimental vs. theoretical grasp quality for both Grasp 1 and 2. Parity line is where experimental grasp quality would be exactly equal to theoretical grasp quality (intercept of 0, slope of 1). Regression line constant term forced to zero. 3-D force portions of grasp wrench set for two different tests shown on right (torque constrained to zero).

implementation, the experimental results lie below the parity line, Fig. 9. Regression analysis with zero intercept shows the best-fit line has a slope of 0.70, which indicates a loss of quality of 30%, on average. Figure 9 shows the 3-D force portions of the feasible grasp wrench set for two representative designs. This shows that the theoretical and experimental 3-D force portions of the grasp wrench are very similar in size and shape, with the experimental sets being contracted due to experimental loss of quality mentioned above. Of note, the optimized best 2N design has a 223% greater experimental grasp quality than the unoptimized naive 2N design for Grasp 1, in agreement with our computational predictions.

4 Discussion

In this work, we have investigated the effect of tendon routings, pulley sizes, and distribution of maximal tendon tensions on the grasp quality of a tendon-driven robotic hand under design constraints. We see that a simple optimization over these design parameters has a very dramatic effect on grasp quality while still satisfying the constraints. We also see that computational predictions can be useful when making design decisions.

We have used radius of largest ball as the grasp quality metric for our analyses since no prior assumption of wrench direction specification was made. If a necessary wrench or set of wrenches is known [33] (e.g., to pick up a heavy object, pull on a cord, or turn a knob) then the analyses could assign a fitness metric to a routing based on that task specification, using a procedure similar to that used in Ref. [17]. The optimization could then be based on that metric. In addition, any other grasp quality metric based on kinetostatic performance (such as the volume of the grasp wrench set [13]) could be used to optimize a tendon-driven hand under constraints.

Our demonstration of this design methodology only used two grasps, but an optimization over a larger set of necessary grasps would generally be desirable for complex research and commercial applications. For instance, two common two-finger grasps for anthropomorphic hands are key pinch and opposition pinch. However, these grasps would ideally be optimized for different sized objects as well.

As in a previous study which utilized a single finger of the same design [20], we only analyzed and constructed routings where the tendons routed around every joint that they passed (i.e., that the structure matrix is pseudo-triangular, as in Ref. [25]) and where there were only two sizes of pulleys that could be chosen. Routings can be designed where tendons pass through the center of joints [34], or where moment arms can have many feasible magnitudes. This opens up the design space even more, and exhaustive searches like the ones we performed in this study may not be feasible. In addition, tendon-driven fingers or manipulators with more than 3 degrees of freedom will tend to suffer from the curse of dimensionality in the design space, and a designer may have to use various optimization algorithms [19] in a search for a very good design which could then be chosen for physical implementation. Alternatively, a designer could define a handful of feasible, physically-realizable routings, and then use this computational optimization to determine the best one to implement.

It should be recognized that the optimization methodology we used in this study does not guarantee the global optimum of grasp qualities. We optimized the pulley sizes only on the best designs determined by the grasp quality with large pulleys. It is possible that another routing which was not initially the best could possibly be optimized over the pulley sizes and outperform the other optimized design. The same is true of the tension-optimizing step. Our methodology produced very good results but cannot guarantee a global optimum based on our methodologies.

We calculated grasp quality based on the wrenches that the fingers could exert on the object. In order to control for other factors such as finger slippage and noise in the system, we fixed the fingers to the object. However, this will not in general represent a realistic use of the hand, and therefore these other factors (such as the ability to resist rather than apply wrenches) would need to be tested in the design of a practical dexterous hand.

Friction was a significant factor in our experiment, especially for the tendons at the last joint that had to wrap around as many as 12 pulleys. This high number of pulleys was necessary to ensure total reconfigurability. Fingers for a commercial robotic hand under constraints (such as a dexterous prosthetic hand) could use these computational methods to design routings where very few pulleys are necessary, and hence the friction could be reduced.

Moreover, the 30% reduction in grasp quality compared with predictions due to frictional loss and other experimental error can partly be explained by the fact that the grasp quality metric used was the "worst case scenario" (i.e., the magnitude of weakest wrench). This would result in the grasp quality being lowered by one or more of many sources of friction loss, small controller errors, or positioning errors of the load cell or fingers, and be similar to a "max error" operator. The experimental volume of the

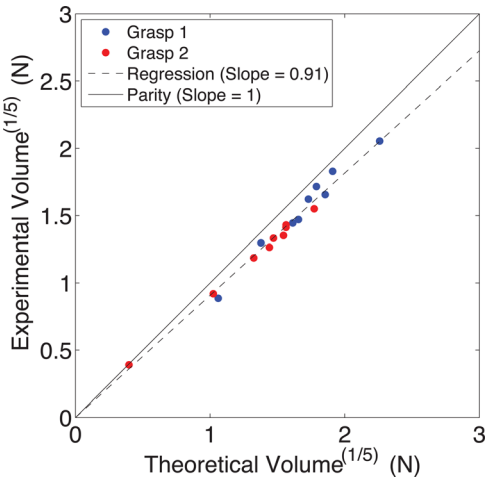

Fig. 10 Experimental vs. predicted volumes of grasp wrench sets

grasp wrench set, which can be viewed as an approximation of the average wrench that can be produced by the fingers, is much more consistent with predictions with a slope of 0.91, as shown in Fig. 10. This could be viewed as an "average error" operator, instead of the worst-case error we report above. We plotted the volume to the one-fifth power to linearly scale the volume for visual inspection and fair comparison with Fig. 9, whose units are in Newtons.

We have investigated grasp quality in this paper, but there are many other considerations that go into the design of a robotic hand. Other significant considerations are the effectiveness of control algorithms, passive stiffness characteristics, sensitivity to friction and positioning errors, and maximal finger velocities. We acknowledge that grasp quality is only one piece of the design puzzle for optimized robotic hands.

This work is also easily extended to the case of underactuated hands. These hands are simpler to design and control, and current users of prosthetic hands can only transfer a few reliable signals to the hand. This limited control bandwidth currently restricts the applicability of these results to prosthetic hands at the current stage of neural interface development. However, as the number of reliable neural or cortical signals from amputees increases, the market for dexterous prosthetic hands will increase dramatically.

This study also gives us insight into the anatomy of the human hand. The human hand's tendon routing is very asymmetric, the distribution of maximal tendon tensions is extremely skewed, and the magnitudes of the moment arms vary widely. In the index finger, the smallest muscle is only 10% of the strength of the largest muscle, the magnitude of the smallest moment arm is approximately 10% of that of the largest moment arm, and it utilizes one less tendon than a 2N design [35]. In fact, our optimized results show that *none* of the optimized designs had much symmetry. We feel that the biological inspiration from these parameter adjustments can be used in the design of tendon-driven robotic systems to maximize performance.

Acknowledgment

The authors gratefully acknowledge the help of Dr. Jason Kutch and Manish Kurse in providing the data acquisition routine for the experimental procedure and also for their helpful comments.

References

[1] Jacobsen, S., Iversen, E., Knutti, D., Johnson, R., and Biggers, K., 1986, "Design of the Utah/MIT Dextrous Hand," 1986 IEEE International Conference on Robotics and Automation. Proceedings, pp. 1520–1532.

[2] Salisbury, J. K., and Craig, J. J., 1982, "Articulated Hands: Force Control and Kinematic Issues," Int. J. Robot. Res., **1**(1), p. 4.

[3] Kochan, A., 2005, "Shadow Delivers First Hand," Ind. Robot, **32**(1), pp. 15–16.

[4] Grebenstein, M., Albu-Schaffer, A., Bahls, T., Chalon, M., Eiberger, O., Friedl, W., Gruber, R., Haddadin, S., Hagn, U., and Haslinger, R., 2011, "The DLR Hand Arm System," Robotics and Automation (ICRA), 2011 IEEE International Conference Shanghai, China, pp. 3175–3182.

[5] Ambrose, R. O., Aldridge, H., Askew, R. S., Burridge, R. R., Bluethmann, W., Diftler, M., Lovchik, C., Magruder, D., and Rehnmark, F., 2000, "Robonaut: Nasa's Space Humanoid," IEEE Intell. Syst. Appl., **15**(4), pp. 57–63.

[6] Jau, B. M., 1995, "Dexterous Telemanipulation With Four Fingered Hand System,", Proceedings of the IEEE International Conference on Robotics and Automation, Vol. 1, pp. 338–343 vol. 1.

[7] Massa, B., Roccella, S., Carrozza, M. C., and Dario, P., 2002, "Design and Development of an Underactuated Prosthetic Hand," Proceedings of the ICRA'02, IEEE International Conference on Robotics and Automation, Vol. 4, pp. 3374–3379.

[8] Lin, L. R., and Huang, H. P., 1996, "Mechanism Design of a New Multifingered Robot Hand," Proceedings of the IEEE International Conference on Robotics and Automation, Vol. 2, pp. 1471–1476.

[9] Kawasaki, H., Komatsu, T., and Uchiyama, K., 2002, "Dexterous Anthropomorphic Robot Hand With Distributed Tactile Sensor: Gifu Hand II," IEEE/ASME Trans. Mechatron., **7**(3), pp. 296–303.

[10] Namiki, A., Imai, Y., Ishikawa, M., and Kaneko, M., 2003, "Development of a High-Speed Multifingered Hand System and Its Application to Catching," Proceedings of the IEEE/RSJ International Conference on Intelligent Robots and Systems, IEEE, Vol. 3, pp. 2666–2671.

[11] Yamano, I., and Maeno, T., 2005, "Five-Fingered Robot Hand Using Ultrasonic Motors and Elastic Elements," Proceedings of the 2005 IEEE International Conference on Robotics and Automation, IEEE, pp. 2673–2678.

[12] Gaiser, I., Schulz, S., Kargov, A., Klosek, H., Bierbaum, A., Pylatiuk, C., Oberle, R., Werner, T., Asfour, T., and Bretthauer, G., 2008, "A New Anthropomorphic Robotic Hand," 8th IEEE-RAS International Conference on Humanoid Robots, IEEE, pp. 418–422.

[13] Miller, A. T., and Allen, P. K., 1999, "Examples of 3d Grasp Quality Computations," IEEE International Conference on Robotics and Automation, Vol. 2.

[14] Miller, A. T., and Allen, P. K., 2004, "Graspit! A Versatile Simulator for Robotic Grasping," IEEE Rob. Autom. Mag., **11**(4), pp. 110–122.

[15] Feijóo, R. S., Cornellà, J., Garzón, M. R., and Industrials, 2006, Universitat Politècnica de Catalunya. Institut d'Organització i Control de Sistemes, *Grasp quality measures*, Institut d'Organització i Control de Sistemes Industrials.

[16] Borst, C., Fischer, M., and Hirzinger, G., 2003, "Grasping the Dice by Dicing the Grasp," Proceedings of the IEEE/RSJ International Conference on Intelligent Robots and Systems (IROS, 2003), Vol. 4.

[17] Fu, J. L., and Pollard, N. S., 2006, "On the Importance of Asymmetries in Grasp Quality Metrics for Tendon Driven Hands," IEEE/RSJ International Conference on Intelligent Robots and Systems, pp. 1068–1075.

[18] Pollard, N. S., and Gilbert, R. C., 2002, "Tendon Arrangement and Muscle Force Requirements for Human-Like Force Capabilities in a Robotic Finger," Proceedings Of the IEEE International Conference on Robotics and Automation, Vol. 4, pp. 3755–3762.

[19] Inouye, J. M., Kutch, J. J., and Valero-Cuevas, F. J., 2012, "A Novel Synthesis of Computational Approaches Enables Optimization of Grasp Quality of Tendon-Driven Hands," IEEE Trans. Rob. Autom., **28**(4), pp. 958–966.

[20] Inouye, J. M., Kutch, J. J., and Valero-Cuevas, F. J., 2013, *Optimizing the Topology of Tendon-Driven Fingers: Rationale, Predictions and Implementation*, Springer Tracts in Advanced Robotics (STAR) series, Balasubramanian, R., and Santos, V. J., Eds., Springer, Heidelberg, Germany, (in press).

[21] Ferrari, C., and Canny, J., 1992, "Planning Optimal Grasps," Proceedings of the IEEE International Conference on Robotics and Automation, IEEE, pp. 2290–2295.

[22] Yu, Z., 2013, "An Efficient Algorithm For a Grasp Quality Measure," IEEE Trans. Rob. Autom., **29**(2), pp. 579–585.

[23] Valero-Cuevas, F. J., 2005, "A Mathematical Approach to the Mechanical Capabilities of Limbs and Fingers," Prog. Motor Control, **629**, pp. 619–633.

[24] Barber, C. B., Dobkin, D. P., and Huhdanpaa, H., 1996, "The Quickhull Algorithm for Convex Hulls," ACM Trans. Math. Softw., **22**(4), pp. 469–483.

[25] Lee, J. J., and Tsai, L. W., 1991, "The Structural Synthesis of Tendon-Driven Manipulators Having a Pseudotriangular Structure Matrix," Int. J. Robot. Res., **10**(3), p. 255.

[26] Butterfafl, J., Grebenstein, M., Liu, H., and Hirzinger, G., 2001, "DLR-Hand II: Next Generation of a Dextrous Robot Hand," Proceedings of the IEEE International Conference on Robotics and Automation, Vol. 1, pp. 109–114.

[27] Santos, V. J., Bustamante, C. D., and Valero-Cuevas, F. J., 2009, "Improving the Fitness of High-Dimensional Biomechanical Models via Data-Driven Stochastic Exploration," IEEE Trans. Biomed. Eng., **56**(3), pp. 552–564.

[28] Finotello, R., Grasso, T., Rossi, G., and Terribile, A., 1998, "Computation of Kinetostatic Performances of Robot Manipulators With Polytopes," Proceedings of the IEEE International Conference on Robotics and Automation, pp. 3241–3246.

[29] Ou, Y. J., and Tsai, L. W., 1993, "Kinematic Synthesis of Tendon-Driven Manipulators With Isotropic Transmission Characteristics," ASME J. Mech. Des., **115**(4), p. 884–891.

[30] Ou, Y. J., and Tsai, L. W., 1996, "Isotropic Design of Tendon-Driven Manipulators," ASME J. Mech. Des.,**118**(3), pp. 360–366.

[31] Tsai, L. W., 1995, "Design of Tendon-Driven Manipulators," ASME J. Mech. Des., **117**(B), pp. 80–86.
[32] Murray, R. M., and Sastry, S. S., 1994, *A mathematical introduction to Robotic Manipulation*, CRC Press, Boca Raton, FL.
[33] Borst, C., Fischer, M., and Hirzinger, G., "Grasp Planning: How to Choose a Suitable Task Wrench Space," Proceedings of the IEEE International Conference on Robotics and Automation, pp. 319–325.
[34] Grebenstein, M., Chalon, M., Hirzinger, G., and Siegwart, R., 2010, "Antagonistically Driven Finger Design for the Anthropomorphic DLR Hand Arm System," Proceedings of the IEEE-RAS International Conference on Humanoid Robots (HUMANOIDS).
[35] Valero-Cuevas, F. J., Towles, J. D., and Hentz, V. R., 2000, "Quantification of Fingertip Force Reduction in the Forefinger Following Simulated Paralysis of Extensor and Intrinsic Muscles," J. Biomech., **33**(12), pp. 1601–1609.